Published in final edited form as:
Nucl Med Biol. 2007 February ; 34(2): 165–171.

Long-circulating liposomes radiolabeled with [^{18}F]fluorodipalmitin ([^{18}F]FDP)

Jan Marik[‡], **Michaelann S. Tartis**[‡], **Hua Zhang**[‡], **Jennifer Y. Fung**, **Azadeh Kheirolomoom**, **Julie L. Sutcliffe**, and **Katherine W. Ferrara**[*]
Department of Biomedical Engineering, University of California Davis, Davis CA 95616

Abstract

Synthesis of a radiolabeled diglyceride 3-[^{18}F]fluorodipalmitoyl-1,2-glycerol (^{18}F-fluorodipalmitin, [^{18}F]FDP) and its potential as a reagent for radiolabeling long-circulating liposomes were investigated. The incorporation of ^{18}F into the lipid molecule was accomplished by nucleophilic substitution of *p*-toluenesolfonyl moiety with a decay corrected yield of 43 ± 10% (n = 12). Radiolabeled long-circulating PEG-coated liposomes were prepared using a mixture of DPPC, cholesterol, DSPE-PEG2000 (61:30:9) and [^{18}F]FDP with a decay corrected yield of 70 ± 8% (n = 4). PET imaging and biodistribution studies were performed with free [^{18}F]FDP and liposome incorporated [^{18}F]FDP. Freely-injected [^{18}F]FDP had the highest uptake in the liver, spleen and lungs. Liposomal [^{18}F]FDP remained in blood circulation at near constant levels for at least 90 minutes, with a peak concentration near 2.5% ID/cc. The use of radiolabeled diglyceride [^{18}F]FDP for radiolabeling of long-circulating liposomes was described. Since [^{18}F]FDP was incorporated into the phospholipid bi-layer it could potentially be used for radiolabeling a variety of possible lipid based drug carriers. Introduction

Keywords

liposome; positron emission tomography; fluorine-18; [^{18}F]fluorodipalmitin; [^{18}F]FDP

Liposomes are vesicles composed of one or more concentric phospholipid bi-layers and such vesicles have been widely investigated as possible drug carriers [1,2]. Prolonged blood circulation of the liposomes is achieved with the addition of a polyethylene glycol (PEG) coating, which efficiently minimizes their removal by macrophages of the reticuloendothelial system [3–6]. Liposomes with various target-specific ligands attached to their surface are being investigated for targeted drug delivery [1,2,7]. Liposomes labeled with radioisotopes such as ^{99m}Tc, ^{186}Re, ^{67}Ga, ^{111}In, and ^{18}F were previously employed to study the biodistribution of different types of liposomes in various animal models using scintigraphy, SPECT and PET. The radionuclides ^{99m}Tc, ^{186}Re, ^{67}Ga, and ^{111}In for SPECT imaging were attached to the liposome surface using chelators, covalently linked to lipid soluble anchors [8], or encapsulated inside the liposome hydrophilic cavity [9–14]. Incorporation of ^{18}F for PET trafficking of long-circulating liposomes was previously achieved by encapsulation of 2-[^{18}F]fluoro-2-deoxy-D-glucose ([^{18}F]FDG) during liposome preparation [15] and therefore the biodistribution kinetics

Corresponding Author: Katherine W. Ferrara, Department of Biomedical Engineering, 451 East Health Sciences Drive, University of California, Davis, Davis, CA 95616-5294, Tel: 530 754-9436, Fax: 530 754-5739, email: kwferrara@ucdavis.edu.
‡J. M., M. S. T. and H. Z. contributed equally to the completion of this work.

were determined both by the liposome and the content. Such studies have been shown to be useful in developing an understanding the effect of size or charge has on the biodistribution of long-circulating stealth liposomes [16]. Vesicles larger than 200 nm accumulate in the spleen since their size does not allow them to pass through the walls of the venous sinuses in splenic red pulp tissue [2,17,18]. This has been clearly demonstrated with the PEG-coated [^{18}F]FDG-labeled liposomes; the vesicles smaller than 100 nm remained in the blood pool and were accumulated in the tumor tissue due to the enhanced permeability and retention effect [19, 20]; conversely, liposomes larger then 200 nm accumulated in spleen and the liver [17]. It was also demonstrated that positively-charged liposomes are more likely to aggregate and become serum-bound compared with neutrally or negatively charged liposomes; and *in vivo* tests revealed that liver and spleen uptake was maximal in positively charged liposomes, while the neutral liposomes had minimal uptake [17].

Herein we describe a synthesis of a radiolabeled diglyceride 3-[^{18}F]fluorodipalmitoyl-1,2-glycerol (^{18}F-fluorodipalmitin, [^{18}F]FDP) and its potential as a reagent for radiolabeling long-circulating liposomes. Contrary to radiolabeling with [^{18}F]FDG [15], encapsulated inside the hydrophilic cavity of the liposome, the diglyceride [^{18}F]FDP is incorporated into the phospholipid bi-layer (Figure 1). The incorporation of the marker inside the phospholipid bi-layer provides a more generic approach for labeling a variety of possible drug carriers such as micelles [21–23], acoustically active lipospheres [24] and microbubbles [25–30] as well as a tool for radiolabeling cells for *in vivo* trafficking [31]. Also, unlike [^{18}F]FDG, we hypothesized that free [^{18}F]FDP should not be internalized and metabolized in cells and therefore the radioactive material should not be retained in heart and brain tissues. Hence the images obtained using [^{18}F]FDP labeled liposomes could more closely reflect the biodistribution of long-circulating vesicles.

Materials and Methods

General

The solvents and chemicals were purchased from Aldrich (Milwaukee, WI). The ^{1}H and ^{13}C NMR spectra were recorded using a Bruker Avance 500 spectrometer and the chemical shifts are reported relative to TMS. Analytical reversed-phase HPLC was performed using a Phenomenex Jupiter 5μ C4 300A column (250 × 4.6 mm 5 μm), with 0.05% TFA/acetonitrile 10/90 (v/v), and a flow rate of 1.5 mL/min. ^{18}F-fluoride was produced from the ^{18}O(p,n)^{18}F nuclear reaction on [^{18}O]H_2O (Marshall Isotopes Ltd. Tel Aviv, Israel) using the RDS111 Siemens/CTI cyclotron. Sep-Pak SPE cartridges were obtained from Waters (Milford, MA) and ^{18}F Trap & Release Columns were purchased from ORTG, Inc (Oakdale, TN). The extruder and lipids were purchased from Avanti Polar Lipids Inc. (Alabaster, AL). The size distribution of liposomes was determined using a particle size analyzer Nanotrac NPA150 purchased from Microtrac Inc. (North Largo, FL). The lipid concentration was determined using a Phospholipids B kit purchased from Wako Chemicals, Inc. (Richmond, VA).

Synthesis of 3-tosyl-1,2-dipalmitoyl glycerol (2)

The precursor **2** was prepared according to the previously published procedure [32] from 1,2-dipalmitoyl-*sn*-glycerol (**1**) and 4-toluenesulfonyl chloride. The crude product was subsequently purified by recrystalization from hexane. ^{1}H NMR ($CDCl_3$, 500 MHz) δ 0.81 (t, *J* = 7.0 Hz, 6H, $CH_2C\underline{H}_3$); 1.17–1.25 (bs, 48H, alkyl chains); 1.47–1.51 (bs, 4H, $C\underline{H}_2CH_2CO$); 2.17 (t, 2H, *J* = 7.5 Hz, $CH_2C\underline{H}_2CO$), 2.18 (t, 2H, *J* = 7.5 Hz, $CH_2C\underline{H}_2CO$), 2.39 (s, 3H, Ar-$C\underline{H}_3$); 4.10 (dAB, 2H, *J* = 11.0, 4.5 Hz, $CH_2CHC\underline{H}_2OTs$); 4.11 (dAB, 2H, *J* = 12.0, 5.0 Hz, $C\underline{H}_2CHCH_2OTs$); 5.09 (m, 1H, $CH_2C\underline{H}CH_2OTs$); 7.29 (d, 2H, *J* = 8.0 Hz, Ar$\underline{H}$); 7.72 (d, 2H, *J* = 8.0 Hz, Ar$\underline{H}$). ^{13}C NMR ($CDCl_3$, 125.8 MHz) δ 14.12 ($\underline{C}H_3CH_2$); 21.76 (Ar$\underline{C}H_3$); 22.70 ($CH_3\underline{C}H_2$); 24.81 ($\underline{C}H_2CH_2CO$); 29.1–29.7 (alkyl chains); 31.9

($CH_3CH_2\underline{C}H_2$); 33.96 ($CH_2\underline{C}H_2CO$); 34.04 ($CH_2\underline{C}H_2CO$); 61.39 ($CH_2CH\underline{C}H_2OTs$); 67.30 ($\underline{C}H_2CHCH_2OTs$); 68.29 ($CH_2\underline{C}HCH_2OTs$); 128.00 (Ar); 129.94 (Ar); 132.19 (Ar); 145.18 (Ar); 172.64 (CO); 173.06 (CO)

Radiochemical synthesis of 3-[^{18}F]fluoro-1,2-dipalmitoyl glycerol, [^{18}F]FDP (3)

The [^{18}F]fluoride anion was captured on an ion exchange ^{18}F Trap & Release Column and eluted with 1.0 mL of acetonitrile solution containing 6% water, 5 mg 4,7,13,16,21,24-hexaoxa-1,10-diazabicyclo[8.8.8]hexacosane (K222), and 1 mg K_2CO_3. The acetonitrile was evaporated under a gentle stream of nitrogen at 100 ºC. The remaining water was removed from the K222/K[^{18}F]F complex by azeotropic distillation with acetonitrile (3 × 1 mL). The content of the vial was dissolved in anhydrous acetonitrile (0.35 mL) and transferred into a suspension of **2** (5.5 mg) in anhydrous acetonitrile (0.5 mL). The reaction mixture was heated to 100 ºC for 20 minutes and allowed to cool to room temperature for 5 min. The solution was aspirated into a syringe containing chloroform (6 mL) and passed through a Silica Plus Sep-Pak cartridge previously treated with acetonitrile (10 mL) and air (10 mL). The eluant was evaporated using a gentle stream of nitrogen and the product was dissolved in hexane (6 mL). The crude product was purified by chromatography using three Silica Plus Sep-Pak cartridges previously treated with hexane (20 mL) and air (10 mL). The product was eluted with a 50:1 (v/v) hexane/ethyl acetate mixture and the solvent was evaporated under a gentle stream of nitrogen. The HPLC retention time was 9.4 min and purity 99%.

Preparation of [^{18}F]FDP -labeled liposomes

The solution of **2** in CH_2Cl_2 was added to a solution of 1,2-dipalmitoyl-*sn*-glycero-3-phosphocholine (DPPC, 1.6 mg, 0.0022 mmol), cholesterol (0.4 mg, 0.001 mmol), and 1,2-distearoyl-*sn*-glycero-3-phosphoethanolamine-*N*-[methoxy(polyethyleneglycol)-2000] ammonium salt (DSPE-PEG2000, 0.9 mg, 0.00032 mmol) (61:30:9) in $CHCl_3$ and the solvent was evaporated using a stream of nitrogen. Dulbecco's phosphate-buffered saline (0.6 mL) was added and the suspension was sonicated at 50 ºC for 10 minutes. The resulting vesicles were extruded through a series of polycarbonate membranes at 50–60 ºC (11 passes through 200 μm diameter pores, then 11 passes through 100 μm diameter pores). The extruded liposomes were purified using gel chromatography on Sephadex G-75 with PBS as an eluant. The liposomal size distribution and the phospholipid concentration were measured.

Biodistribution studies

All animal experiments were conducted under a protocol approved by the University of California, Davis Animal Use and Care Committee, Davis, CA. Male Fischer 344 rats (Harlan, Indianapolis, IN) were anesthetically induced with 3.5% isofluorane and maintained at 2.0–2.5%, after which they were catheterized to ensure proper tail vein injection. Bolus injections composed of approximately 1 mCi (range 0.559–1.254 mCi) of either [^{18}F]FDP-labeled liposomes in isotonic solution or free [^{18}F]FDP in ethanol were administered as PET scans were initiated, using a manually-controlled injection timed to occur uniformly over 1 minute. Two acquisition protocols for the microPET Focus (Concorde Microsystems, Inc.) were used. The first acquisition protocol consisted of a 90-minute continuous bed motion scan to ensure the entire rat could be imaged. The second acquisition protocol consisted of a static scan of the abdomen to record dynamic time activity data on select organs. Full body image reconstructions were obtained using maximum a posteriori (MAP) and maximum intensity projections (MIPs) created with ASIPro software (CTI Molecular Imaging). MAP reconstructed images of the abdomen were used to obtain quantitative activity levels in each organ of interest as a function of time. Time activity curves (TACs) are expressed as percent injected dose per cubic centimeter (%ID/cc) with the mean and standard deviation presented. These measurements

were obtained with region of interest (ROI) analysis using ASIPro software (CTI Molecular Imaging).

Results and Discussion

Preparation of radiolabeled liposomes

The starting material for the precursor preparation (Scheme 1) was a naturally occurring diglyceride 1,2-dipalmitoyl-*sn*-glycerol **1** (1,2-dipalmitin, DP). The incorporation of ^{18}F into the molecule was accomplished by nucleophilic substitution of *p*-toluenesolfonyl moiety in acetonitrile at reflux. Although the tosylate **2** is not soluble in acetonitrile at room temperature, it dissolves readily at higher temperatures. The yield of the nucleophilic substitution is strongly affected by the amount of K[^{18}F]F/K222 and K_2CO_3 present in the reaction mixture. The reaction produced a favorable yield of [^{18}F]FDP **3** when 5 mg of K222 and 1 mg of K_2CO_3 were used to elute the [^{18}F]fluoride anion from ion exchange column. The yield was substantially lower when larger amounts of eluting reagents were present. The unreacted [^{18}F]fluoride was removed using a Silica SepPak cartridge and the precursor **2** was removed by chromatography using three Silica SepPak cartridges to provide **3** with a decay corrected radiochemical yield of 43 ± 10% (n = 12) in 60 minutes with a specific activity greater than 3.0 Ci/mmol. As demonstrated by RP-HPLC analysis, the two step SPE purification provided the fluorinated lipid **3** free of the starting precursor **2,** which could potentially affect the stability of subsequently formed liposomes if present.

Radiolabeled long-circulating PEG coated liposomes were prepared using a mixture of DPPC, cholesterol, DSPE-PEG2000 (61:30:9) and **3**. The DSPE-PEG2000 was incorporated into the lipid mixture to provide PEG coating for maximum circulation time. The lipids were dried and subsequently rehydrated using PBS, and then sonicated at a temperature above the phase transition. The resulting vesicles were extruded through a series of filters to provide unilamellar liposomes smaller than 100 nm [33,34]. The sized liposomes were purified on gel chromatography to remove non-incorporated **3**. The radiolabeled liposomes were obtained with a decay corrected radiochemical yield of 70 ± 8% (n = 4) decay corrected in 53 minutes after the end of the synthesis of **3**. The liposomal specific activity was measured as 23.9 ± 4.2 mCi (n = 4) per 1 mg of total lipid content, with lipid content determined by the Phospholipids B assay. Assuming that all lipids are contained in spherical unilamellar liposomes and that the surface area of the phospholipid head is approximately 65×10^{-2} nm^2, the number of liposomes generated from 1 mg of phospholipid mixture is 2.5×10^{13} thus the specific activity of the [^{18}F]FDP-radiolabeled liposomes is 1 mCi per 10^{12} liposomes.

[^{18}F]FDP-radiolabeled liposomes were incubated in PBS for 24 hours at room temperature and the size of the resulting particles was determined to be 45 ± 18 nm (n = 5). Non-radiolabeled liposomes were used as a standard sample for the *in vitro* stability test, assuming that the minute amount of no-carrier-added [^{18}F]FDP does not change the vesicle properties. Since the change in the size distribution of liposomes over time reflects their stability [40], the size distribution of non-radiolabeled liposomes was measured at 1, 2, and 24 hours after preparation. The obtained mean diameter, 29 ± 9 nm (n = 2), was comparable with the size of [^{18}F]FDP-radiolabeled liposomes and did not change over time. We therefore conclude that the [^{18}F]FDP-radiolabeled liposomes are stable *in vitro* for 24 hours.

Biodistribution

Maximum intensity projection images obtained from 90-minute continuous bed motion scans illustrate the full body distribution of free and liposome-encapsulated [^{18}F]FDP (Figure 2). Freely-injected [^{18}F]FDP (n = 5) had the highest uptake in the liver, spleen and lungs. Freely-injected [^{18}F]FDP was also inconsistently taken up in the lungs, where two out of eight scans

revealed discrete regions of high uptake in the lungs. Liposome-encapsulated [^{18}F]FDP (n = 3) circulated in the blood stream for the duration of the scan, highlighting the vasculature in detail in the resulting image.

Quantification of the 90-minute static scans of the abdomen with ROI analysis reinforced these findings and provided a dynamic profile for each [^{18}F]FDP formulation (Figure 3). Freely-injected [^{18}F]FDP (n = 3) showed an initial concentration of 3% ID/cc and was cleared from the blood within a few minutes, followed by a subsequent small peak at 15 minutes, corresponding to a sharp decrease in activity in the liver. The small peak was also observed in the kidney and lung, likely reflecting the blood content within these organs. The greatest concentration of free [^{18}F]FDP was observed in the liver, 5.5 %ID/cc on average. Free [^{18}F]FDP also rapidly accumulated in the spleen early in the scan to a concentration of 4.2% ID/cc, with activity decreasing after roughly 15 minutes. Liposomal [^{18}F]FDP (n = 3) remained in blood circulation at near constant levels for at least 90 minutes, with a peak concentration near 2.5% ID/cc. In addition, liposomal [^{18}F]FDP quickly reached a steady state in the liver, spleen, kidney, and lungs, which was maintained throughout the scan reflecting the activity within the vasculature of these organs. However, the activity associated with the liposome-incorporated [^{18}F]FDP in the lungs was higher than other organs and higher than expected (2% ID/cc). Alveolar macrophages, present in high numbers within the rat, may be responsible for the elevated retention of radiolabeled liposomes in the lungs. The diameter of the extruded liposomes was determined to be 45 ± 18 nm and the diameter of the largest detected liposome was 210 nm, therefore liposomal particles were not expected to be mechanically-lodged within the pulmonary capillaries.

As previously discussed, free [^{18}F]FDG leaking from radiolabeled liposomes [17] could account for the higher uptake of radioactive material in the myocardium and brain tissues. Free fatty acids and triglycerides are another major source of energy for the heart muscle, hence, radiolabeled fatty acids, such as 9,10-[^{18}F]fluorostearic acid, 2-[^{18}F]fluorostearic acid, 16-[^{18}F]fluorohexadecanoic acid, and 17-[^{18}F]fluoroheptadecanoic acid [35], [ω-^{11}C]palmitic acid [36,37], 16-[^{18}F]fluoro-4-thia-palmitate [38], and 14-[^{18}F]fluoro-6-thia-heptadecanoic acid [39] were used for PET imaging of alterations in fatty acid metabolism in the myocardium. However, we did not observe elevated retention of radioactivity in the myocardium (Figure 2). Free [^{18}F]FDP did not show substantial brain or heart uptake whereas images obtained with [^{18}F]FDP-liposomes showed the brain vasculature and minimal internalization in the heart muscle, noting that both ventricles and both atria are clearly separated. The low retention of free [^{18}F]FDP in heart tissues where β-oxidation of fatty acid is a source of energy suggests that the [^{18}F]FDP is not metabolized within the heart. Under normal dietary conditions, the metabolism of lipids such as diglycerides includes transport of the lipids to the liver, where the lipid molecule is incorporated into lipoproteins and released back to the blood stream for storage in fat. It is reasonable to assume that, in the case of free [^{18}F]FDP, the steep decrease of the activity in the liver and increase of the activity in other organs at 15 minutes after injection was associated with lipoprotein formation and release to the blood stream (Figure 3). The liposome-incorporated [^{18}F]FDP was effectively protected from such metabolic transformation and the activity in the blood pool remained nearly constant (2.5% ID/cc) over the 90 minute scan. The accumulation of free [^{18}F]fluoride in bone is a marker for defluorination of the radiolabeled tracer. However, bone uptake was not detectable in the case of free [^{18}F]FDP or liposome-incorporated [^{18}F]FDP. Also, activity was not detected in the bladder or gut, indicating that the excretion of [^{18}F]FDP or its metabolites *via* renal and hepatobiliary routes is minimal over the duration of the scan (90 min).

Conclusions

We have developed a novel method for radiolabeling liposomes with ^{18}F using the radiolabeled lipid [^{18}F]FDP. In contrast to the previously published approach using FDG encapsulation, the lipid [^{18}F]FDP is incorporated into the phospholipid bi-layer. The *in vivo* imaging data show that the long-circulating liposomes remained in the blood stream for at least 90 minutes and the free [^{18}F]FDP is not metabolized in the myocardium. The incorporation of the no-carrier-added radiolabeled lipid inside the phospholipid bi-layer offers a generic approach to radiolabeling a wide variety of lipid-based drug delivery vehicles.

Acknowledgements

The work was supported by NIH R01 CA 103828. We would like to thank Steve Rendig, Chris Griesemer, for their assistance with PET image acquisition, and Salma Jivan and David Kukis for radionuclide production and Jinyi Qi and Lin Fu for help with image reconstruction.

References

1. Torchilin VP. Recent advances with liposomes as pharmaceutical carriers. Nat Rev Drug Discov 2005;4:145–160. [PubMed: 15688077]
2. Moghimi SM, Hunter AC, Murray JC. Long-circulating and target-specific nanoparticles: theory to practice. Pharmacol Rev 2001;53:283–318. [PubMed: 11356986]
3. Oku N, Tokudome Y, Asai T, Tsukada H. Evaluation of drug targeting strategies and liposomal trafficking. Curr Pharm Des 2000;6:1669–1691. [PubMed: 10974160]
4. Blume G, Cevc G. Liposomes for the sustained drug release in vivo. Biochim Biophys Acta 1990;1029:91–97. [PubMed: 2223816]
5. Klibanov AL, Maruyama K, Torchilin VP, Huang L. Amphipathic polyethyleneglycols effectively prolong the circulation time of liposomes. FEBS Lett 1990;268:235–237. [PubMed: 2384160]
6. Allen TM, Hansen C, Martin F, Redemann C, Yau-Young A. Liposomes containing synthetic lipid derivatives of poly(ethylene glycol) show prolonged circulation half-lives in vivo. Biochim Biophys Acta 1991;1066:29–36. [PubMed: 2065067]
7. Sapra P, Tyagi P, Allen TM. Ligand-targeted liposomes for cancer treatment. Curr Drug Deliv 2005;2:369–381. [PubMed: 16305440]
8. Tilcock C, Ahkong QF, Fisher D. ^{99m}Tc-labeling of lipid vesicles containing the lipophilic chelator PE-DTTA: effect of tin-to-chelate ratio, chelate content and surface polymer on labeling efficiency and biodistribution behavior. Nucl Med Biol 1994;21:89–96. [PubMed: 9234269]
9. Bao A, Goins B, Klipper R, Negrete G, Phillips WT. ^{186}Re-liposome labeling using ^{186}Re-SNS/S complexes: in vitro stability, imaging, and biodistribution in rats. J Nucl Med 2003;44:1992–1999. [PubMed: 14660726]
10. Bao A, Goins B, Klipper R, Negrete G, Phillips WT. Direct ^{99m}Tc labeling of pegylated liposomal doxorubicin (Doxil) for pharmacokinetic and non-invasive imaging studies. J Pharmacol Exp Ther 2004;308:419–425. [PubMed: 14610219]
11. Bao A, Goins B, Klipper R, Negrete G, Mahindaratne M, Phillips WT. A novel liposome radiolabeling method using ^{99m}Tc-"SNS/S" complexes: in vitro and in vivo evaluation. J Pharm Sci 2003;92:1893–1904. [PubMed: 12950007]
12. Phillips WT, Rudolph AS, Goins B, Timmons JH, Klipper R, Blumhardt R. A simple method for producing a technetium-99m-labeled liposome which is stable in vivo. Int J Rad Appl Instrum B 1992;19:539–547. [PubMed: 1399684]
13. Woodle MC. ^{67}Gallium-labeled liposomes with prolonged circulation: preparation and potential as nuclear imaging agents. Nucl Med Biol 1993;20:149–155. [PubMed: 8448567]
14. Essien H, Hwang KJ. Preparation of liposomes entrapping a high specific activity of $^{111}In^{3+}$-bound inulin. Biochim Biophys Acta 1988;944:329–336. [PubMed: 3179293]
15. Oku N, Tokudome Y, Tsukada H, Kosugi T, Namba Y, Okada S. In vivo trafficking of long-circulating liposomes in tumour-bearing mice determined by positron emission tomography. Biopharm Drug Dispos 1996;17:435–441. [PubMed: 8830978]

16. Moghimi SM, Porter CJ, Muir IS, Illum L, Davis SS. Non-phagocytic uptake of intravenously injected microspheres in rat spleen: influence of particle size and hydrophilic coating. Biochem Biophys Res Commun 1991;177:861–866. [PubMed: 2049107]

17. Oku N. Delivery of contrast agents for positron emission tomography imaging by liposomes. Adv Drug Deliv Rev 1999;37:53–61. [PubMed: 10837726]

18. Chen LT, Weiss L. The role of the sinus wall in the passage of erythrocytes through the spleen. Blood 1973;41:529–537. [PubMed: 4688868]

19. Maeda H, Sawa T, Konno T. Mechanism of tumor-targeted delivery of macromolecular drugs, including the EPR effect in solid tumor and clinical overview of the prototype polymeric drug SMANCS. J Control Release 2001;74:47–61. [PubMed: 11489482]

20. Maeda H. The enhanced permeability and retention (EPR) effect in tumor vasculature: the key role of tumor-selective macromolecular drug targeting. Adv Enzyme Regul 2001;41:189–207. [PubMed: 11384745]

21. Nasongkla N, Shuai X, Ai H, Weinberg BD, Pink J, Boothman DA, Gao J. cRGD-functionalized polymer micelles for targeted doxorubicin delivery. Angew Chem Int Ed Engl 2004;43:6323–6327. [PubMed: 15558662]

22. Shuai X, Ai H, Nasongkla N, Kim S, Gao J. Micellar carriers based on block copolymers of poly (epsilon-caprolactone) and poly(ethylene glycol) for doxorubicin delivery. J Control Release 2004;98:415–426. [PubMed: 15312997]

23. Dabholkar RD, Sawant RM, Mongayt DA, Devarajan PV, Torchilin VP. Polyethylene glycol-phosphatidylethanolamine conjugate (PEG-PE)-based mixed micelles: some properties, loading with paclitaxel, and modulation of P-glycoprotein-mediated efflux. Int J Pharm 2006;315:148–157. [PubMed: 16616818]

24. Unger EC, McCreery TP, Sweitzer RH, Caldwell VE, Wu Y. Acoustically active lipospheres containing paclitaxel: a new therapeutic ultrasound contrast agent. Invest Radiol 1998;33:886–892. [PubMed: 9851823]

25. Kinoshita M, Hynynen K. A novel method for the intracellular delivery of siRNA using microbubble-enhanced focused ultrasound. Biochem Biophys Res Commun 2005;335:393–399. [PubMed: 16081042]

26. Kinoshita M, Hynynen K. Intracellular delivery of Bak BH3 peptide by microbubble-enhanced ultrasound. Pharm Res 2005;22:716–720. [PubMed: 15906165]

27. Bloch SH, Dayton PA, Ferrara KW. Targeted imaging using ultrasound contrast agents. Progess and opportunities for clinical and research applications. IEEE Eng Med Biol Mag 2004;23:18–29. [PubMed: 15565796]

28. Dayton PA, Pearson D, Clark J, Simon S, Schumann PA, Zutshi R, Matsunaga TO, Ferrara KW. Ultrasonic analysis of peptide- and antibody-targeted microbubble contrast agents for molecular imaging of αvβ3-expressing cells. Mol Imaging 2004;3:125–134. [PubMed: 15296677]

29. Klibanov AL. Ligand-carrying gas-filled microbubbles: ultrasound contrast agents for targeted molecular imaging. Bioconjug Chem 2005;16:9–17. [PubMed: 15656569]

30. Shortencarier MJ, Dayton PA, Bloch SH, Schumann PA, Matsunaga TO, Ferrara KW. A method for radiation-force localized drug delivery using gas-filled lipospheres. IEEE Trans Ultrason Ferroelectr Freq Control 2004;51:822–831. [PubMed: 15301001]

31. Ma B, Hankenson KD, Dennis JE, Caplan AI, Goldstein SA, Kilbourn MR. A simple method for stem cell labeling with fluorine 18. Nucl Med Biol 2005;32:701–705. [PubMed: 16243645]

32. Auteri SC, Cameron DW. Mixed carboxylate sulphonate esters of glycerol. Aust J Chem 1977;30:2487–2492.

33. Berger N, Sachse A, Bender J, Schubert R, Brandl M. Filter extrusion of liposomes using different devices: comparison of liposome size, encapsulation efficiency, and process characteristics. Int J Pharm 2001;223:55–68. [PubMed: 11451632]

34. Olson F, Hunt CA, Szoka FC, Vail WJ, Papahadjopoulos D. Preparation of liposomes of defined size distribution by extrusion through polycarbonate membranes. Biochim Biophys Acta 1979;557:9–23. [PubMed: 95096]

35. Knust EJ, Kupfernagel C, Stocklin G. Long-chain F-18 fatty acids for the study of regional metabolism in heart and liver; odd-even effects of metabolism in mice. J Nucl Med 1979;20:1170–1175. [PubMed: 317095]

36. Guiducci L, Jarvisalo M, Kiss J, Nagren K, Viljanen A, Naum AG, Gastaldelli A, Savunen T, Knuuti J, Salvadori PA, Ferrannini E, Nuutila P, Iozzo P. [^{11}C]palmitate kinetics across the splanchnic bed in arterial, portal and hepatic venous plasma during fasting and euglycemic hyperinsulinemia. Nucl Med Biol 2006;33:521–528. [PubMed: 16720244]

37. Hostetler ED, Fallis S, McCarthy TJ, Welch MJ, Katzenellenbogen JA. Improved methods for the synthesis of [ω-^{11}C]palmitic acid. J. Org. Chem 1998;63:1348–1351.

38. DeGrado TR, Kitapci MT, Wang S, Ying J, Lopaschuk GD. Validation of ^{18}F-Fluoro-4-Thia-Palmitate as a PET Probe for Myocardial Fatty Acid Oxidation: Effects of Hypoxia and Composition of Exogenous Fatty Acids. J Nucl Med 2006;47:173–181. [PubMed: 16391202]

39. Ebert A, Herzog H, Stocklin GL, Henrich MM, DeGrado TR, Coenen HH, Feinendegen LE. Kinetics of 14(R,S)-fluorine-18-fluoro-6-thia-heptadecanoic acid in normal human hearts at rest, during exercise and after dipyridamole injection. J Nucl Med 1994;35:51–56. [PubMed: 8271060]

40. Lasic, DD. Liposomes: from Physics to Applications. Amsterdam: Elsevier; 1993.

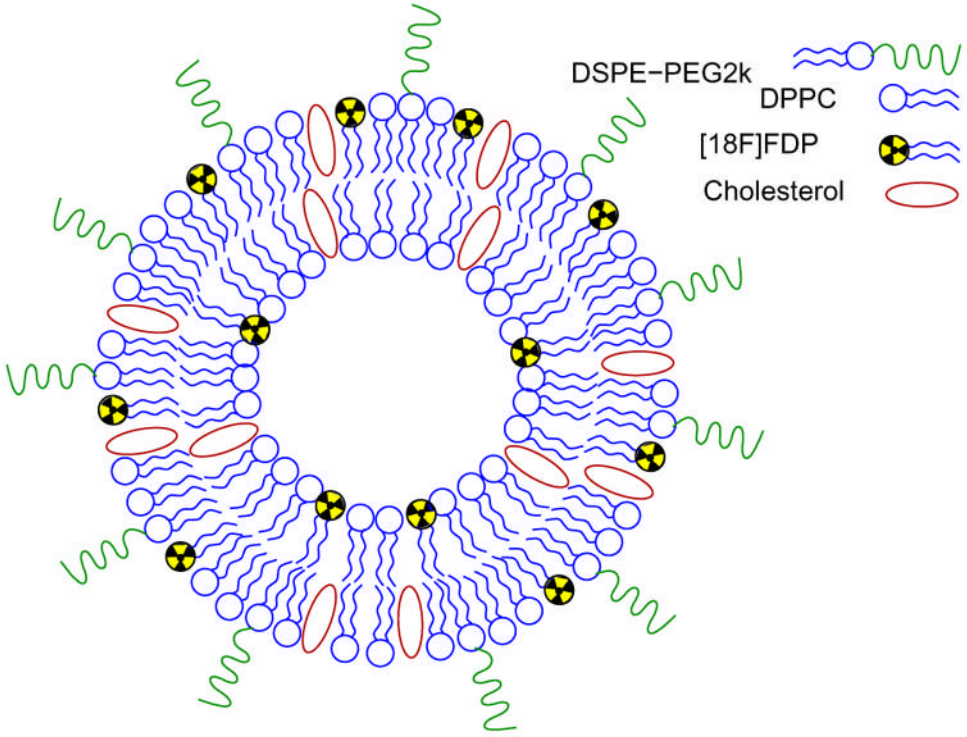

Figure 1.
[^{18}F]FDP radiolabeled liposome.

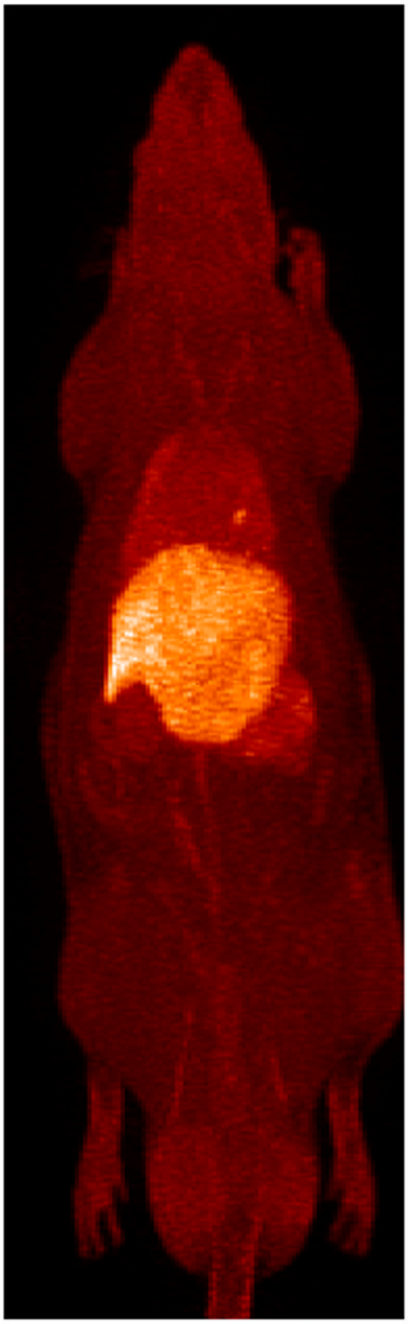

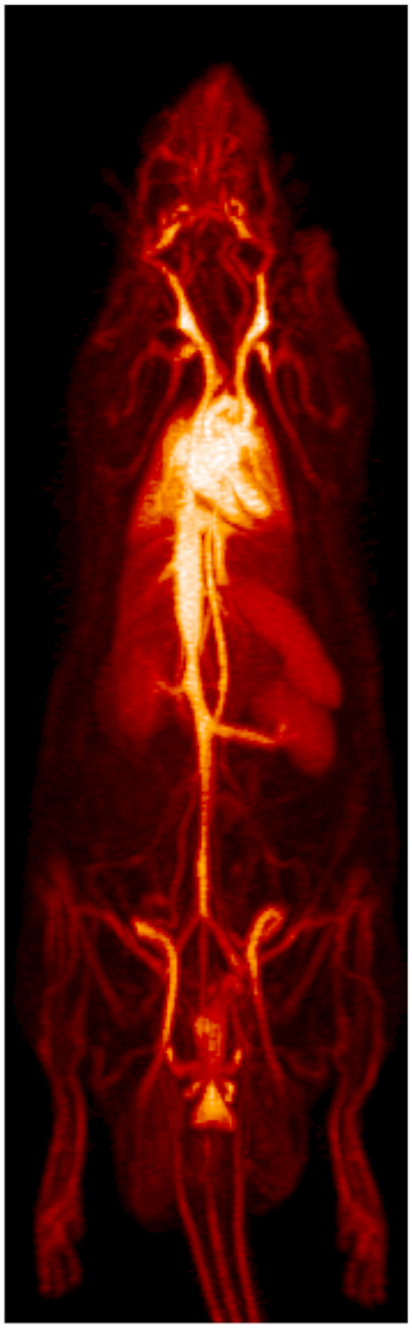

Figure 2.
Full body maximum intensity projections (MIP) for [^{18}F]FDP and [^{18}F]FDP-liposome in a rat model. A MIP of free [^{18}F]FDP is shown in the left image with uptake in liver, spleen and lungs. The right image shows a MIP of liposomal [^{18}F]FDP which remains circulating in the blood for the duration of the 90-minute scan. Animals were anesthetically induced with 3.5% isofluorane and maintained at 2.0–2.5%. Bolus injections were composed of approx 1 mCi of either [^{18}F]FDP-labeled liposomes or free [^{18}F]FDP and administered through a tail vein catheter.

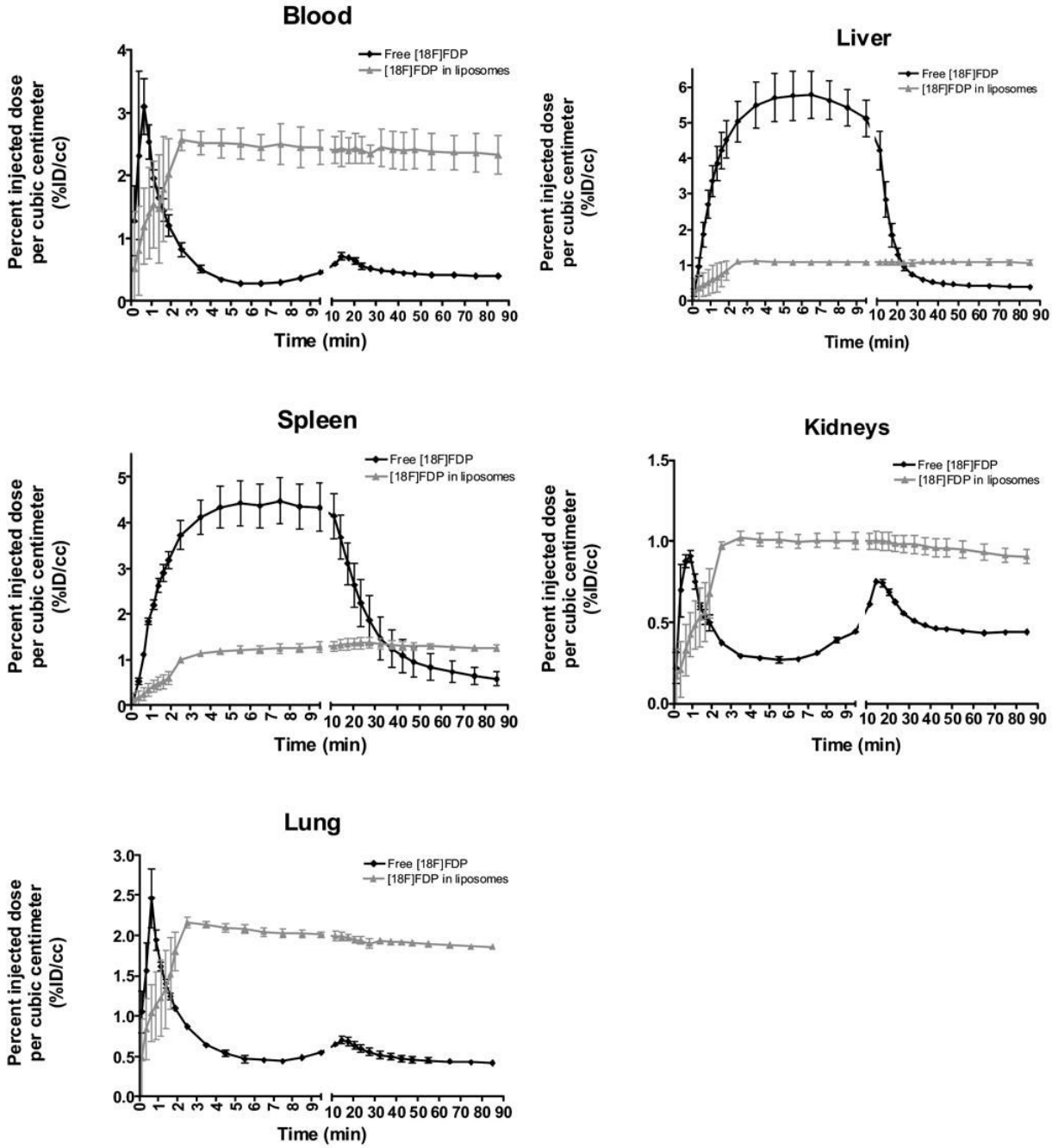

Figure 3.

Time activity curves: Activity levels are quantified over 90 minutes as percent injected dose per cubic centimeter of blood for free and liposomal [^{18}F]FDP.

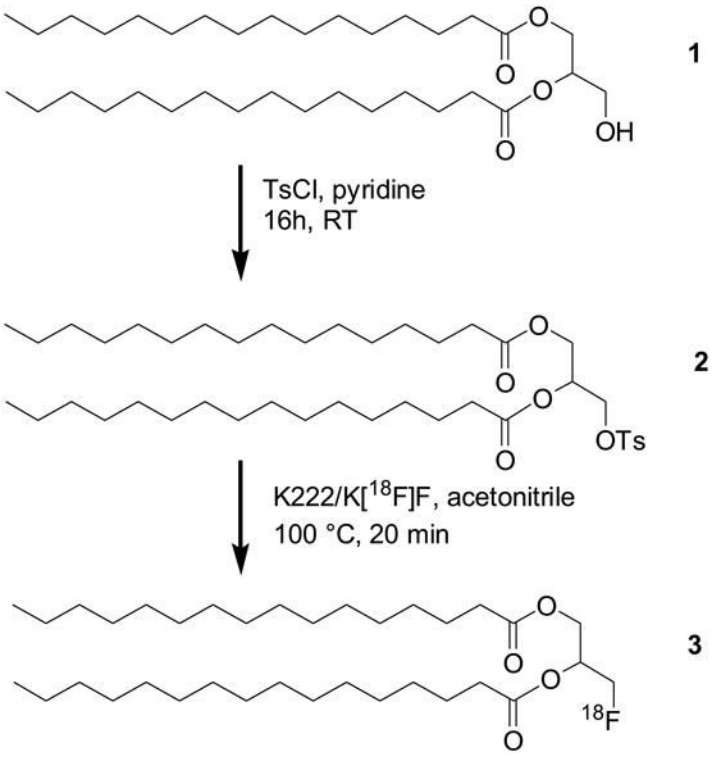

Scheme 1.
Radiochemical synthesis of [^{18}F]FDP **3**.